$-(2/k)\langle\varphi_{k,l}|V_{op}'|(\psi_{k,l}-\varphi_{k,l})\rangle$ because of the use of Eq. (13) in calculating second-order results. This is verified in Table IV where these effects have been estimated. The estimates listed under "higher-order terms" are believed to be accurate to within 5% except for $k=0.80$. It is not surprising that there is more uncertainty at $k=0.80$ since the inelastic threshold occurs at $k=0.866$. The constant part of the energy denominator of Eq. (18) is quite small at $k=0.80$ and the approximation of Eq. (18) is less accurate than it is for larger values of $\frac{1}{2}k^2+\epsilon_n$. For example, $\frac{1}{2}k^2+\epsilon_n=-0.18$ at $k=0.80$ and -0.320 at $k=0.60$. Near the inelastic threshold we might expect better results to be obtained with use of a set of excited states corresponding to single-particle excitations which could describe inelastic processes, unlike the present excited states, all of which are in the continuum. That is, we could use hydrogenic states including $2s$, $2p$, etc., and continuum states. This set of states could also describe resonances below the inelastic threshold.[17]

The estimates of $\langle\varphi_{k,l}|V_{op}'|(\psi_{k,l}-\varphi_{k,l})\rangle$ based on the method of Sec. II are somewhat uncertain, and it would be desirable to obtain more information concerning the functional form of V_{op}'.

The separate contributions to δ_l from excited states with $l=0$ and $l=1$ in Table II and including higher-order effects compare satisfactorily with the corresponding values listed by Schwartz.[20]

[0] C. Schwartz, Phys. Rev. 126, 1015 (1962).

One further consideration is the omission of excited states with $l\geq 3$. A detailed discussion of the convergence in l for second-order energies and for phase shifts has been given by Schwartz.[20] In the present calculations the contributions from second-order terms with $l\geq 3$ are estimated to be small but not completely negligible. However, it is estimated that the second-order terms with $l\geq 3$ will be reduced significantly by the third-order l-changing ladder diagrams containing one pair of intermediate states with $l\geq 3$ and another pair with $l=0$, 1, or 2.

Note added in proof. These calculations did not include the effect of the nonorthogonality of the scattering solutions to the $1s$ state beyond the Hartree-Fock term in Eq. (9). Inclusion of this correction might account for the discrepancy for $k=0.80$ in Table IV.

The numerical results obtained in this calculation indicate the feasibility of applying this optical potential approach to other atoms, and calculations are planned for many S-state atoms.

ACKNOWLEDGMENTS

I am grateful to the late Professor M. E. Rose for his support and encouragement. I also wish to acknowledge helpful discussions with Professor R. A. Ferrell and with Dr. M. Rho, Dr. A. Ron, Dr. H. Schmidt, and Dr. F. Schwabel. I am also grateful to Professor A. Batson and his staff at the Computer Science Center of the University of Virginia for help with the calculations.

PHYSICAL REVIEW VOLUME 171, NUMBER 1 5 JULY 1968

Hyperfine Structure in the Millimeter Spectrum of Hydrogen Sulfide: Electric Resonance Spectroscopy on Asymmetric-Top Molecules

R. E. CUPP, R. A. KEMPF, AND J. J. GALLAGHER
Martin Marietta Corporation, Orlando, Florida

(Received 14 July 1967; revised manuscript received 21 February 1968)

The magnetic hyperfine structure of the $1_{-1}\leftrightarrow 1_1$ rotational transition of H_2S has been fully resolved in a millimeter electric-resonance spectrometer. The hyperfine components have been measured with an accuracy of 2 parts in 10^{10}. The hyperfine coupling constants are determined to be

$C_{ss}=$ 16 726±30 Hz (spin-spin),
$C_{1_{10}}=-16\,239\pm10$ Hz (spin-rotation constant for 1_1 rotational state),
$C_{1_{01}}=-15\,885\pm10$ Hz (spin-rotation constant for 1_{-1} rotational state).

The center frequency of the rotational transition is determined to be $\nu_0=168,762,762,373\pm20$ Hz. Several sources of frequency shift and line distortion have been investigated. Seven rotational transitions of hydrogen sulfide have been observed, four of them in the electric-resonance spectrometer. The electric-resonance technique has been extended to a wavelength of 813 μ by observation of the $4_0\leftrightarrow 4_2$ rotational transition of H_2S.

INTRODUCTION

THE first electric-resonance experiment in the millimeter-wavelength region was performed[1] in 1963 on the diatomic molecule Li^6F^{19}. This investigation, performed on a collaborative basis, raised several interesting questions which could not be answered during the short time allowed for the experiment. Thus, it was left unanswered whether sufficient spectral purity of the originating source was available to observe Ramsey patterns[2] in the millimeter region, and, if such

[1] L. Wharton, W. Klemperer, L. P. Gold, R. Strauch, J. J. Gallagher, and V. E. Derr, J. Chem. Phys. 38, 1203 (1963).

[2] N. F. Ramsey, Phys. Rev. 76, 996 (1949).

patterns were observable, whether they could contribute to further resolution of hyperfine structure as observed in the single-resonator case. In addition, concern was expressed on the feasibility of observing zero-field rotational transitions which would greatly simplify the calculation of the hyperfine structure. Consideration was given to the extension of the molecular-beam technique to molecules other than diatomic molecules which are usually observed in beam studies. Finally, it was questioned whether standing waves are necessary for separated field observations in the millimeter region or whether traveling waves, provided by horn-lens systems, are adequate for observation of Ramsey patterns; the latter capability would greatly simplify the experimental techniques.

With the apparatus employed for the present investigation, solutions to these questions have been obtained. Observation of Ramsey patterns has been reported previously[3] for the asymmetric-top molecule H_2S. The magnetic hyperfine structure of the $1_{-1} \leftrightarrow 1_1$ rotational transition of H_2S at 168.7 GHz has been fully resolved in zero-C-field transitions (or in fields sufficiently small that zero-field perturbation calculations can be employed); complete resolution was not possible in the single-field excitation scheme. The hyperfine components have been measured with an accuracy of 2 parts in 10^{10}, a figure not achieved by other millimeter-spectroscopy methods, and molecular-beam studies have been performed at frequencies as high as 369 GHz. In addition, Ramsey patterns have been observed under excitation by horn-lens systems.

The advantages of millimeter-molecular-beam spectroscopy can now be realized. The sensitivity, high resolution, and ability to investigate high temperature and unstable molecules are highly desirable features of the spectrometer. In this paper, the resolution of the $1_{-1} \leftrightarrow 1_1$ rotational transition of H_2S is described.

HYPERFINE STRUCTURE THEORY

The hyperfine structure of asymmetric rotors has been the subject of several theoretical investigations. The work of Thaddeus, Krisher, and Loubser[4] is appropriate for the analysis of the hyperfine structure of the rotational transitions of hydrogen sulfide. This theory, as applicable to the H_2S^{32} millimeter observations, is briefly described here. It has been independently discussed by Huiszoon.[5]

The hydrogen sulfide molecule has a C_{2v} symmetry and a $^1\Sigma$ ground state. The hyperfine structure is due only to the two protons, so no quadrupole-moment contributions are present. The Hamiltonian is then given by

$$H=\sum_g A_g(J_g-L_g)^2+\frac{e\mu_N}{c}\sum_{i,K} g_K r_{iK}^{-3}\mathbf{r}_{iK}\times(\mathbf{v}_i-\gamma_K\mathbf{v}_K)\cdot\mathbf{I}_K$$
$$-\frac{e\mu_N}{c}\sum_{K,L\neq K} Z_L g_K r_{LK}^{-3}[\mathbf{r}_{LK}\times(\mathbf{v}_L-\gamma_K\mathbf{v}_K)]\cdot\mathbf{I}_K$$
$$+\mu_N^2\sum_{K,L\neq K} g_K g_L r_{LK}^{-3}[(\mathbf{I}_L\cdot\mathbf{I}_K)-3r_{LK}^{-2}(\mathbf{I}_L\cdot\mathbf{r}_{LK})(\mathbf{I}_K\cdot\mathbf{r}_{LK})], \quad (1)$$

where J_g and L_g are, respectively, the components of the total angular momentum excluding nuclear spins and the electronic orbital angular momentum along the principal axis of inertia of the molecule. The A_g are the rotational constants given in terms of the principal moments of inertia. The index i refers to the electrons, with charges $-e$ and positions and velocities $\mathbf{r}_i$ and $\mathbf{v}_i$, with respect to the molecular center of mass. The indices K and L refer to the nuclei, with masses M_K, charges eZ_K, and spins I_K, and $\gamma_K=(1-Z_K M_P/g_K M_K)$. The nuclear g factors are defined so that the magnetic dipole moment operator is $\boldsymbol{\mu}_K=g_K\mu_N\mathbf{I}_K$ with μ_N the nuclear magneton. M_p is the proton mass, c is the velocity of light, and $\mathbf{r}_{ij}=\mathbf{r}_i-\mathbf{r}_j$.

The first term in Eq. (1) is the Hamiltonian for rigid rotation of the nuclear frame. The second term is the energy of interaction between the nuclear dipole moments and the currents due to electronic motion. The third term is the interaction energy between the nuclear dipole moments and the currents due to the nuclear motion, while the last term is the magnetic dipole-dipole interaction of the nuclei.

In the case of hydrogen sulfide, the rotational energy is more than 3×10^6 times larger than the largest hyperfine term ($\sim$48 kHz), so that terms off-diagonal in the rotational states are negligible. Thaddeus *et al.*[4] have reduced the perturbation problem to the averaging of the Hamiltonian over a given asymmetric rotor wave function. The averaging process then gives the hfs energy as a function of $\mathbf{J}$, $\mathbf{I}_K$, and the coupling constants.

Considering the last term of the Hamiltonian, the spin-spin interaction, the averaging process yields the energy expression

$$H_{ss}=[g_L g_K\mu_N^2 d_J/J(2J-1)]\{\tfrac{3}{2}[(\mathbf{I}_L\cdot\mathbf{J})(\mathbf{I}_K\cdot\mathbf{J})+(\mathbf{I}_K\cdot\mathbf{J})(\mathbf{I}_L\cdot\mathbf{J})]-(\mathbf{I}_L\cdot\mathbf{I}_K)\mathbf{J}^2\}, \quad (2)$$

in which

$$d_J=2\sum_g(\langle J_g^2\rangle R_{gg})/[(J+1)(2J+3)], \quad (3)$$

and the $\langle J_g^2\rangle$ are the average values of the square of the components of J along the principal inertial axes of the molecule. The R_{gg} are the diagonal elements of the dyadic

$$\mathbf{R}=r_{KL}^{-5}(-3\mathbf{r}_{LK}\mathbf{r}_{LK}+r_{LK}^2\mathbf{1}). \quad (4)$$

The quantity d_J can be evaluated from the molecular geometry. This fact will be used to obtain a spin-spin

[3] R. G. Strauch, R. E. Cupp, V. E. Derr, and J. J. Gallagher, Proc. IEEE 54, 506 (1966).
[4] P. Thaddeus, L. C. Krisher, and J. H. N. Loubser, J. Chem. Phys. 40, 257 (1964).
[5] C. Huiszoon, doctoral thesis, De Katholieke Universiteit, Nijmegen, Holland (unpublished).

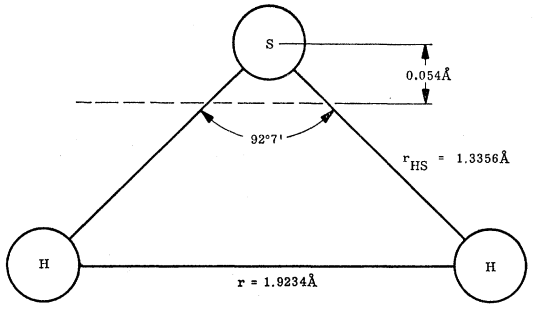

FIG. 1. Geometry of hydrogen sulfide molecules.

constant for each rotational state of an H_2S transition in terms of r_{pp}^{-3}, where r_{pp} is the proton-proton distance of H_2S.

The third term of Eq. (1) produces a nuclear $\mathbf{I}\cdot\mathbf{J}$ interaction which contributes to the hfs in first order and for the Kth nucleus can be written as

$$H_{\text{nucl }\mathbf{I}\cdot\mathbf{J}}=\mathbf{I}_K\cdot\mathbf{N}\cdot\mathbf{J},$$

where $\mathbf{N}$ is a tensor with components in the principal axis system of the molecule given by

$$N_{g'g}=-(2eg_K\mu_N A_g/hc)\times\sum_{L\neq K}Z_L r_{LK}^{-6}[\mathbf{r}_{LK}\cdot(\mathbf{r}_L-\gamma_K\mathbf{r}_K)\delta_{gg'}-(r_{LK})_g(\mathbf{r}_L-\gamma_K\mathbf{r}_K)_{g'}]. \quad (5)$$

Following the averaging of $\mathbf{N}$ over an asymmetric rotor wave function, the resulting energy expression is

$$H_{\text{nucl }\mathbf{I}\cdot\mathbf{J}}=[\sum_g\langle J_g^2\rangle N_{gg}/J(J+1)]\mathbf{I}_K\cdot\mathbf{J}. \quad (6)$$

The components of N can be calculated from Eq. (5) and the molecular geometry, but the contribution from the second term of Eq. (1) which is off-diagonal in first order requires more information than is available on the excited-state electronic wave functions. The contribution of this term, the interaction of the nuclei with the orbital motion of the electrons, is second-order, depending upon the cross terms in the rotational Hamiltonian, proportional to J_gL_g which connect excited electronic states to the $^1\Sigma$ ground state. For the Kth nucleus, the electronic $\mathbf{I}\cdot\mathbf{J}$ interaction is then given as

$$H_{\text{elec }\mathbf{I}\cdot\mathbf{J}}=\mathbf{I}_K\cdot\mathbf{E}\cdot\mathbf{J}, \quad (7)$$

in which $\mathbf{E}$ is a tensor fixed in the molecular frame with components

$$E_{g'g}=2(e/c)g_K\mu_N A_g\times\sum_{i,n}\frac{\langle 0|L_g|n\rangle\langle n|\rho_{g'}|0\rangle+\langle 0|\rho_{g'}|n\rangle\langle n|L_g|0\rangle}{W_n-W_0}. \quad (8)$$

The index n is summed over all excited electronic states, while

$$\boldsymbol{\rho}=r_{iK}^{-3}\mathbf{r}_{iK}\times(\mathbf{v}_i-\gamma_K\mathbf{v}_K).$$

When the average of Eq. (7) is included in the total $\mathbf{I}\cdot\mathbf{J}$ interaction, then the result for the Kth nucleus is

$$H_{\mathbf{I}\cdot\mathbf{J}}=[\sum_g\langle J_g^2\rangle(N_{gg}+E_{gg})/J(J+1)]\mathbf{I}_K\cdot\mathbf{J}. \quad (9)$$

Since the effects of N_{gg} and E_{gg} on the constant in Eq. (9) are not separable and because of the lack of knowledge of the components E_{gg}, it is necessary that the constant for the $\mathbf{I}\cdot\mathbf{J}$ interaction be determined from the experimental data for each rotational state. The sum of Eqs. (2) and (9) is then the hyperfine Hamiltonian for hydrogen sulfide. For H_2S, the hfs is due only to the two equivalent protons, so that the appropriate representation for calculation of the energy is (I_1,I_2,I,J,F,M_F). Then, $\mathbf{I}=\mathbf{I}_1+\mathbf{I}_2$ and $C\mathbf{I}_1\cdot\mathbf{J}+C\mathbf{I}_2\cdot\mathbf{J}=C\mathbf{I}\cdot\mathbf{J}$ where C is the spin-rotation constant of Eq. (9). The hyperfine expression is then:

$$H_{\text{total}}=\frac{g_H^2\mu_N^2(d_J)_{pp}}{2I(2I-1)J(2J-1)}\times[3(\mathbf{I}\cdot\mathbf{J})^2+\tfrac{3}{2}(\mathbf{I}\cdot\mathbf{J})-I^2J^2]+C\mathbf{I}\cdot\mathbf{J}. \quad (10)$$

The requirement that the total wave function be symmetric or antisymmetric on exchange of equivalent nuclei restricts the values of I which can occur in a given rotational state. For H_2S, the antisymmetric rotational levels have $I=1$ while the symmetric rotational levels have $I=0$. Thus, the $1_{01}\leftrightarrow 1_{10}$ rotational transition at 168.7 GHz will consist of six hyperfine components, since $I=1$ for the two rotational levels involved, but transitions, such as the $2_{11}\leftrightarrow 2_{20}$ at 216.7 GHz for $I=0$, are void of hyperfine structure. The hyperfine structure of the $1_{01}\leftrightarrow 1_{10}$ transition is investigated in this paper.

The constant $(d_J)_{pp}$ can now be simplified from Eq. (3) and the geometry of H_2S. The diagonal components R_{gg} of the tensor Eq. (4) can be obtained from consideration of the H_2S geometry as given in Fig. 1 with the distance r_{LK} chosen as the proton-proton distance r. The distances given in the figure are determined from the H_2S moments of inertia of Edwards, Moncur, and

TABLE I. Rotational parameters of H_2S.

	Rotational states	
	1_{01}	1_{10}
$E(\kappa)$	$\kappa-1$	$\kappa+1$
$\partial E/\partial\kappa$	1	1
$\langle J_a^2\rangle$	0	1
$\langle J_b^2\rangle$	1	1
$\langle J_c^2\rangle$	1	0
$(d_J)_{pp}$	$(R_{bb}+R_{cc})/5=+\frac{2}{5}(1/r_{pp}^3)$	$(R_{aa}+R_{bb})/5=-\frac{1}{5}(1/r_{pp}^3)$
C_{ss}	$\frac{1}{5}g_H^2\mu_N^2(1/r_{pp}^3)$	$-\frac{1}{10}g_H^2\mu_N^2(1/r_{pp}^3)$

$\langle J_a^2\rangle=\frac{1}{2}[J(J+1)+E(\kappa)-(\kappa+1)\partial E(\kappa)/\partial\kappa]$
$\langle J_b^2\rangle=\partial E(\kappa)/\partial\kappa$
$\langle J_c^2\rangle=\frac{1}{2}[J(J+1)-E(\kappa)+(\kappa-1)\partial E(\kappa)/\partial\kappa]$

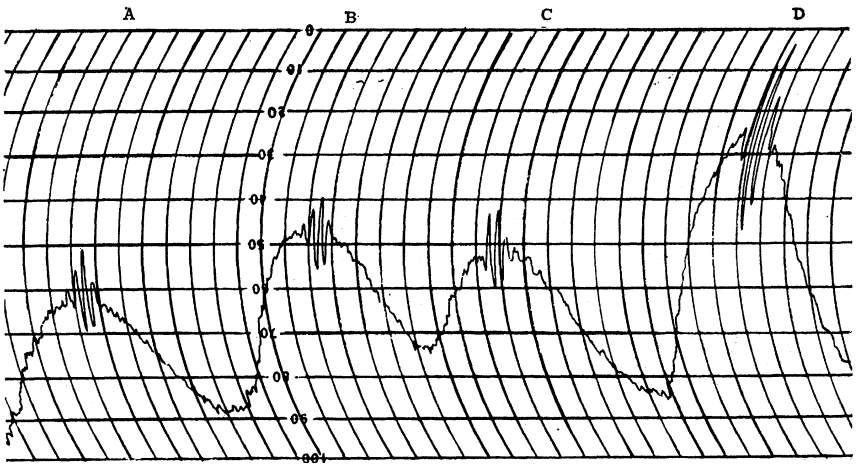

FIG. 2. Partially resolved hyperfine structure of the $1_{01} \leftrightarrow 1_{10}$ rotational transition of hydrogen sulfide.

Snyder.[6] The $\langle J_g^2 \rangle$ and $E(\kappa)$, given in Table I, are employed to obtain $(d_J)_{pp}$ and C_{ss}, also given for the 1_{01} and 1_{10} levels in Table I. The hyperfine energy for the two levels 1_{10} and 1_{01} can then be expressed as

$$H_{1_{10}} = -\tfrac{1}{10} g_H^2 \mu_N^2 (1/r^3)[3(\mathbf{I}\cdot\mathbf{J})^2 + \tfrac{3}{2}(\mathbf{I}\cdot\mathbf{J}) - I^2 J^2] + C_{1_{01}} \mathbf{I}\cdot\mathbf{J} \quad (11a)$$

and

$$H_{1_{01}} = \tfrac{1}{5} g_H^2 \mu_N^2 (1/r^3)[3(\mathbf{I}\cdot\mathbf{J})^2 + \tfrac{3}{2}(\mathbf{I}\cdot\mathbf{J}) - I^2 J^2] + C_{1_{01}} \mathbf{I}\cdot\mathbf{J}. \quad (11b)$$

These two equations, with the three constants $g_H^2 \mu_N^2 (1/r^3)$, $C_{1_{01}}$ and $C_{1_{10}}$, are employed to fit the six hyperfine components of the $1_{-1} \leftrightarrow 1_1$ rotational transition at 168.7 GHz.

EXPERIMENTAL TECHNIQUES

The electric-resonance techniques employed in this investigation have been discussed in general elsewhere.[3] For the observations on the $1_{-1} \leftrightarrow 1_1$ line at 168.7 GHz, the third harmonic of a phase-locked OKI 55V10 klystron is employed. An intermediate klystron at X band is in turn phase locked to the 9400 harmonic of a 1-MHz crystal oscillator. The millimeter signal is continuously tuned through the hydrogen sulfide transition by a motor-driven interpolation oscillator at the X-band frequency of the multiplier chain. This oscillator is a Rohde-Schwarz XUA frequency synthesizer which is continuously checked with a frequency counter driven by the frequency standard. Modulation is provided either by Stark modulation on the plates of the interferometers in the millimeter excitation scheme or by phase modulation on the 5 MHz input to the 5 MHz–120 MHz multiplier amplifier.

The millimeter excitation scheme employs the separated-field method[2] in which two resonators, separated by 27 in. between centers, are used to produce Ramsey interference patterns for the individual hyperfine components. The millimeter resonators are flat-plate Fabry-Perot interferometers which are constructed with low Q values ($\approx$10 000 or less) in order to avoid line-pulling effects in the frequency measurements. The Fabry-Perot plates are constructed by an electroforming process. The hole patterns required for the desired coupling and transmission are calculated,[7] and photographic negatives are prepared. A flat, polished stainless steel plate is coated with a photoresist, photographed and stripped so that the resist remains only where the coupling holes are desired. Electroforming on this plate with nickel or copper produces the plates with holes where the resist has been left. The thin plate, when removed from the stainless-steel mandrel, is then gold plated. The thin films are then stretched over a circular frame to form the interferometer plates.

These thin plates were found to be the most satisfactory for molecular-beam investigations. Films, which employed quartz plates as substrates, were often found to result in spurious effects due to multiple reflections between the plates surfaces.

The Ramsey patterns which are obtained with this apparatus have half widths of 290 Hz for dry ice and acetone temperature (196°K), which is approximately the theoretical limit for this temperature. This is achieved by the use of a moly-permalloy magnetic shield through which the molecular beam passes and in which holes are cut for the two interferometers. Periodic degaussing is required to maintain the 290-Hz linewidth. The achievement of these narrow Ramsey patterns provides the high resolution that is necessary for the H_2S spectrum.

The frequency measurements have been made with two independent frequency standards. A James Knight FS1 100 T crystal oscillator, checked against WWV-B, provides a 1-MHz signal accurate to $\pm 2 \times 10^{10}$; a Hewlett-Packard 5060 A cesium-beam frequency standard was also used with a 5-MHz output and an accuracy

[6] T. H. Edwards, N. K. Mondur, and L. E. Snyder, J. Chem. Phys. 46, 2139 (1967).

[7] W. Culshaw, IRE Trans. Microwave Theory Tech. **MTT-7**, 221 (1959).

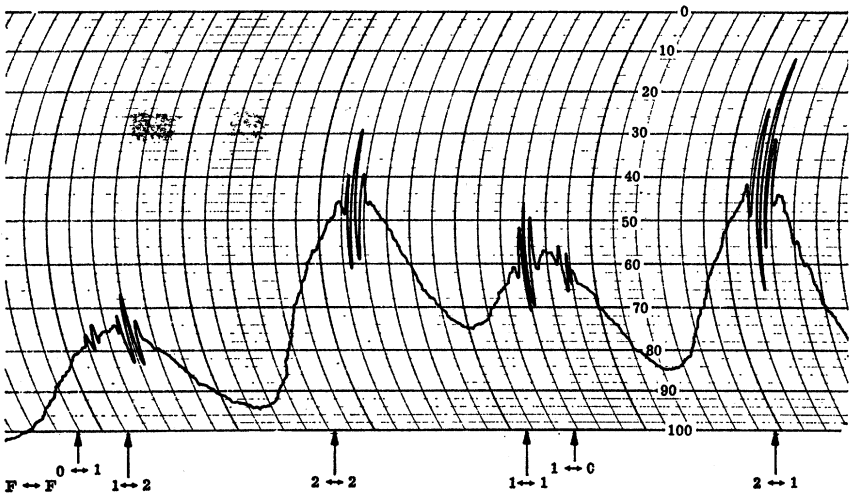

FIG. 3. Hyperfine structure ($1_{01} \leftrightarrow 1_{10}$ transition of H_2S) with six individual Ramsey interference patterns.

of $\pm 2 \times 10^{-11}$. The results obtained with the two standards are indistinguishable.

The cooled source maintains a steady gas flow by means of a Granville-Phillips automatic pressure controller and a Granville-Phillips capacitance manometer. The manometer is used to measure the pressure in the chamber, behind the source, of approximately 2.4 mm Hg relative to the apparatus source chamber. A voltage output is compared to a preset reference in the servo controller. The servo leak valve is thus controlled, maintaining the pressure behind the source slits. The hydrogen sulfide beam is detected by an electron-bombardment–mass-spectrometer system which has been described previously.[3] The mass spectrometer is a conventional Nier-type[8] 60-deg sectoral apparatus. The ion beam, after passing through the mass spectrometer, exits through a 0.020-in. slit and impinges on an ITT FW 141 electron multiplier, the output of which is fed to the lock-in detection system. A modulation rate of 17 Hz is employed. The millimeter power required for these experiments is estimated to be on the order of 10^{-8} W. All measurements require attenuation at the millimeter output to prevent saturation of the transitions.

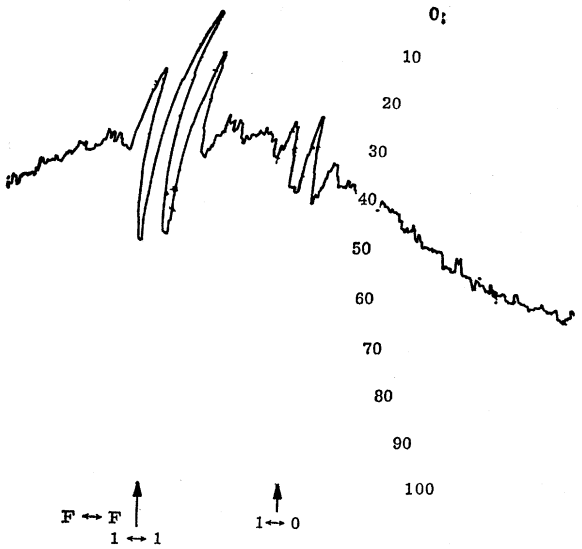

FIG. 4. Ramsey pattern of $F=1 \leftrightarrow 1$ and $F=1 \leftrightarrow 0$ components of 168.7-GHz line of H_2S.

[8] A. O. Nier, Rev. Sci. Instr. 18, 398 (1947).

EXPERIMENTAL RESULTS

In the initial observations on the H_2S hyperfine structure of the $1_{01} \leftrightarrow 1_{10}$ rotational transition, the spectrum was partially resolved into four components. This is shown in Fig. 2, which is a recording of the zero-field transitions. When the observations were performed with a Stark square-wave modulation, the voltages applied to the interferometer plates were switched between zero and a higher voltage, e.g., 1400 V. The resulting spectrum consisted of a zero-field representation and the Stark components appropriate to the applied voltage. If, on the other hand, phase modulation is employed, the observations can be performed in the absence of applied Stark fields. The measured component frequencies employing both modulation schemes are indistinguishable within the accuracy of the experiments. Here it is noted that the "zero-field" observations are made in the presence of the earth's residual magnetic field and any stray electric and magnetic fields. With the magnetic shielding, however, these fields have not been great

TABLE II. Relative intensities for absorption; $1_{01} \leftrightarrow 1_{10}$ transition of H_2S.

$F \rightarrow F'$	Intensity
$0 \rightarrow 0$	0
$1 \rightarrow 1$	2.0
$0 \rightarrow 1$	2.7
$1 \rightarrow 0$	2.7
$1 \rightarrow 2$	3.3
$2 \rightarrow 1$	3.3
$2 \rightarrow 2$	10.0

TABLE III. Observed hfs in $1_{-1} \rightarrow 1_1$. Rotational transition in H_2S^{32}.

$F \leftrightarrow F'$	Observed ν (Hz)	$\Delta\nu$ (Hz)	Calculated ν (Hz)	$\delta\nu$ (Hz) $\nu_{cal}-\nu_{obs}$	$\delta\nu'$ (Hz)
$0 \leftrightarrow 1$	168 762 734 310	3467	168 762 734 296	−14	−17
$1 \leftrightarrow 2$	168 762 737 777	21 744	168 762 737 776	−1	+33
$2 \leftrightarrow 2$	168 762 759 521	15 762	168 762 759 510	−11	−9
$1 \leftrightarrow 1$	168 762 775 283	3667	168 762 775 272	−11	−7
$1 \leftrightarrow 0$	168 762 778 950	18 036	168 762 778 966	+16	−7
$2 \leftrightarrow 1$	168 762 796 986 ±36 Hz		168 762 797 006	+20	−8

enough to distort the spectrum or to prevent the calculation of the spectrum by the field-free representation discussed above. Both $\Delta m_J = \pm 1$ and $\Delta m_J = 0$ transitions have been observed as the Stark components. The $\Delta m_J = 0$ transitions require the use of a pair of Stark plates perpendicular to the interferometer plates.

In Fig. 2, two observations can be made: (1) The single resonator pedestals upon which the Ramsey interference patterns are situated are approximately 8 kHz wide and do not allow the complete resolution of the six hyperfine components which are expected; (2) it will be seen that the intensity ratios of the four resolved components are not compatible with the theoretical intensity ratios. These intensity anomalies could be the result of Majorana transitions among the hyperfine energy levels.

In later observations, further attenuation of the excitation energy has resulted in resolution of the six hyperfine transitions. Figure 3 shows the hyperfine structure with the six individual Ramsey interference patterns. Although, for single-resonator excitation, the width of the line is too broad to permit resolution of the structure, the Ramsey method produces six resonance interference patterns centered at the individual transition frequencies. The center frequencies of these patterns have been measured by the techniques described above. The measurements were conducted over a period of approximately two weeks and were set up each day independently of the experimental arrangement of the previous day. Five measurements of each hyperfine frequency were made, two with the James Knight standard and three with the H-P cesium-beam apparatus. All measurements agreed within ±2 Hz at X band or ±36 Hz at the 168.7-GHz transition. In Fig. 4, the two components, $F=1 \leftrightarrow 1$ and $F=1 \leftrightarrow 0$, are shown more closely. The strongest component, $F=2 \leftrightarrow 1$, is shown in Fig. 5. It is seen from Table II that the intensities observed in the electric-resonance apparatus do not correspond to the relative theoretical intensities usually observed in absorption. Figure 6.2 of Ref. 5 details the absorption intensities for the $1_{01} \rightarrow 1_{10}$ transitions.

Calculation of the transition frequencies is performed by using Eqs. (11a) and (11b) for the energy levels. Table III shows the observed frequencies of the hyperfine transitions, $F \rightarrow F'$, the splitting between components $\Delta\nu$, the calculated frequencies, and the difference $\nu_{calc}-\nu_{obs}$. The calculated frequencies are obtained from a least-squares fit of the six lines with Eqs. (11a) and (11b). It is seen that all lines are calculated within 20 Hz of the observed value. The constants $C_{1_{01}}$, $C_{1_{10}}$ and $g_H^2\mu_H^2(1/r^3)$, determined in this calculation, are listed in Table IV. If one were to use only the four strongest hyperfine components to determine the three hyperfine constants and then calculate the two weak lines, it is possible to fit all lines within 33 Hz. The differences in the observed frequencies and those calculated in this manner are given as $\delta\nu'$ in Table III. From the least-squares fit, the average center frequency of the rotational transition is calculated to be $\nu_0 = 168\,762\,762\,373$

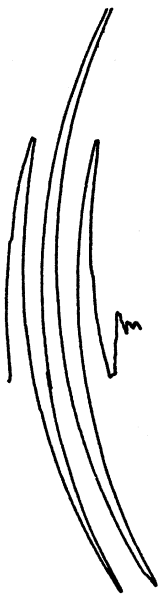

FIG. 5. Ramsey pattern of $F=2 \leftrightarrow 1$ hfs component of $1_{01} \leftrightarrow 1_{10}$ rotational transition of H_2S.

TABLE IV. Hyperfine coupling constants for H_2S.

	(Hz)
C_{ss}	16 726.5±30
$C_{1_{10}}$	−16 239.1±10
$C_{1_{01}}$	−15 885.1±10

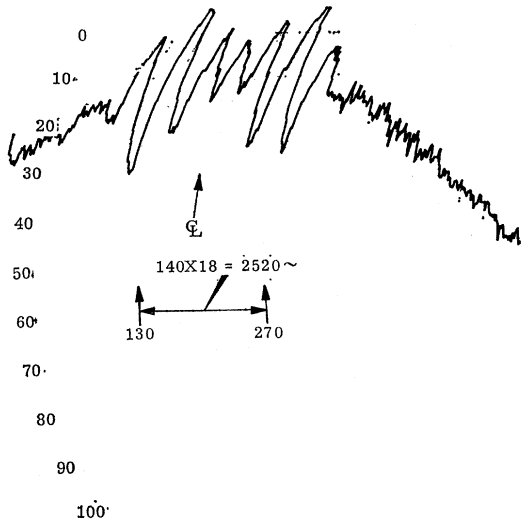

FIG. 6. Zeeman splitting of Ramsey pattern of $F=2 \leftrightarrow 2$ with shield removed.

± 20 Hz. The value of $(1/r^3)$, determined from the experiments, is 13.95×10^{22} cm^{-3} while the value from the geometry, as shown in Fig. 1, is 14.05×10^{22} cm^{-3}.

DISCUSSION

Frequency Shifts and Line Distortions

In support of the frequency measurements of the individual hyperfine components, it has been necessary to investigate various effects which can cause either line distortion or frequency shifts. These effects can, under adverse conditions, cause discrepancies in the frequency measurements in excess of the accuracy of two parts in 10^{10}. The effect of greatest concern in these measurements has been that caused by a relative phase shift between the two separated oscillating fields. It has been shown[9] that, for a 90-deg phase shift between resonators, a frequency shift $\delta\nu \approx 0.55\Delta\nu$ occurs where $\Delta\nu$ is the half-width of the Ramsey pattern. In the transitions considered here, this corresponds to a frequency shift $\delta\nu \approx 160$ Hz. In performing the frequency measurements, the most symmetrical Ramsey pattern corresponding to the two oscillating fields of the same phase was established for each determination. Variation of the phase between resonators caused both distortions and frequency shifts which were observable. For a phase shift large enough to cause a frequency shift of 36 Hz, line distortion was readily evident; this shift and distortion could be established on both sides of the symmetrical pattern by varying the phase shifter back and forth. Thus the accuracy of ± 36 Hz for these measurements appears free of discrepancies from relative phase shifts.

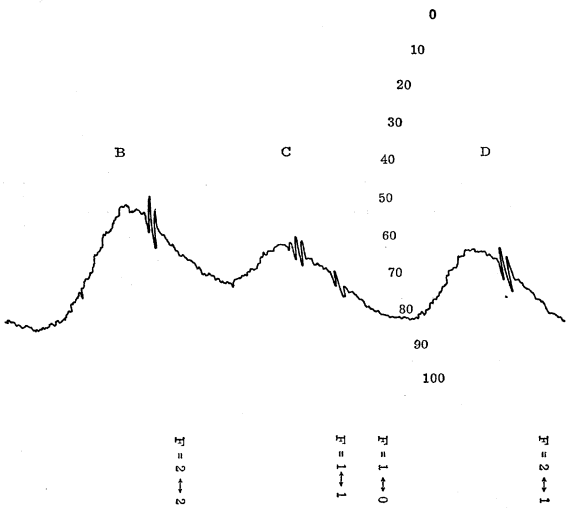

FIG. 7. Hyperfine shift caused by interferometer plates.

Several other causes of frequency shift, discussed by Ramsey and others for rf molecular-beam investigations, have been considered as sources of error in these millimeter-wavelength studies:

(1) Frequency shifts can depend on the amplitude of the oscillating fields in the individual resonators. Saturation effects are quite evident for power levels in excess of 10^{-8} W; however, in the frequency measurements described above, variation of the power level has shown no measurable frequency shifts. While it has been suggested that Majorana transitions could be a cause of the intensity anomalies, some contribution to this effect could result from the difference of electric dipole matrix elements so that some components saturate more readily than others.

(2) The effect of unequal amplitudes of the separate oscillatory fields is not to cause a shift of the midpoint of the resonance but to change the appearance of the resonance. This change could contribute to measurement errors. For each measurement, the amplitudes in each interferometer were adjusted to give the same transition probability. Translation of the interferometers perpendicular to the beam axis allowed the plotting of a standing-wave pattern by the beam detector as the beam passed through electric field maxima and minima. No frequency discrepancies were observed when this field equalizing procedure was followed.

(3) Effects of variations of fixed-field amplitude have been considered negligible. The use of the magnetic shielding in the C-field region nullifies the presence of the earth's magnetic field, as evidenced by the narrow half-widths of the Ramsey patterns. Precautions have been taken to remove or minimize the effects of magnetic materials. With the removal of the magnetic shielding, the individual Ramsey patterns split into doublets as shown in Fig. 6. The doublet splitting is approximately 2.5 kHz for the $F=2 \leftrightarrow 1$ component.

[9] N. F. Ramsey, in *Shapes of Molecular Beam Resonances, Recent Research in Molecular Beams*, edited by I. Estermann (Academic Press Inc., New York, 1959).

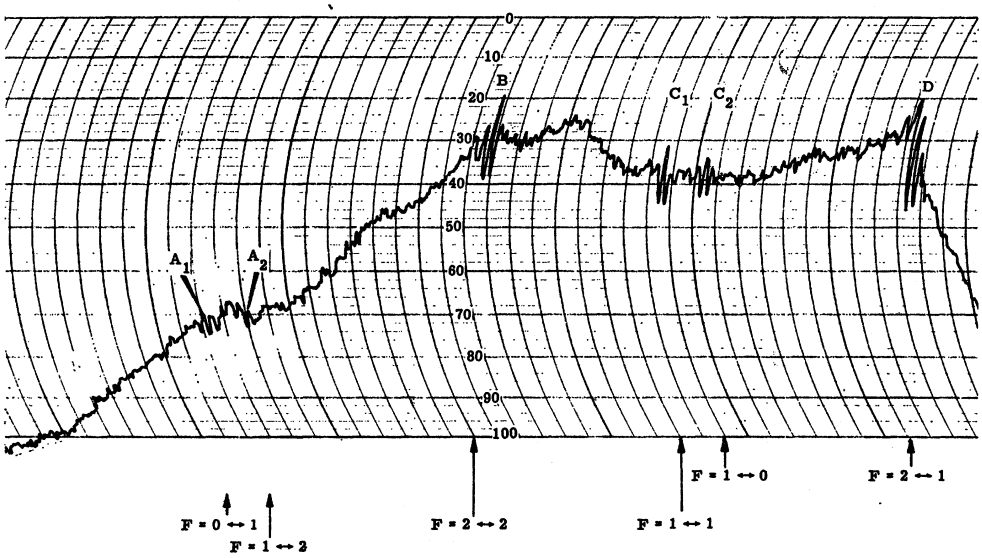

FIG. 8. Horn-lens excitation of the Ramsey system (traveling wave excitation).

(4) The effect of the interferometer on shifting of resonance frequencies has been observed. It has been observed that, under certain interferometer conditions, the single resonator line is considerably shifted relative to the Ramsey patterns. No interferometer changes have been seen to shift the Ramsey patterns. For the cases in which the single resonator response is shifted, it is observed that all hyperfine components are shifted an equal amount, that the shifts are in the same direction, and that power changes (or for that matter, any physical changes) do not alter the frequency shift for a particular interferometer configuration. Frequency pulling by the interferometers can be expected to shift the single resonator lines more so than the Ramsey patterns, but in some cases greater shifts have been observed with interferometers of lower Q. While these resonator effects are presently not understood, it has been demonstrated that they do not cause a measurable shift in the Ramsey patterns that have been employed in the frequency measurements. Figure 7 shows the single-resonator lines shifted with respect to the Ramsey patterns.

Other causes of frequency shifts, discussed in detail by Holloway and Lacey,[10] have been considered for millimeter-wavelength observations, but these are found to be negligible. These effects include second-order Doppler effect, pulling by tails of neighboring lines, Majorana shifts and shifts due to stray electric fields, such as those that might result from the electrostatic deflectors. All of these effects are estimated to be on the order of a few parts in 10^{13}.

[10] J. H. Holloway and R. F. Lacy, in Proceedings of the International Conference on Chronometry, Lausanne, 1964, pp. 319–331 (unpublished).

Horn-Lens Excitation System

The question of whether a millimeter-wavelength Ramsey system could employ a traveling wave technique was investigated by using a pair of horn-lens systems separated by 27 in. A pair of small Stark plates was arranged so that $\Delta m_J = 0$ transitions were observed in the modulation scheme. The resulting hyperfine structure pattern had the single-resonator responses smeared because of the poor collimation of the millimeter-signal relative to that obtained with an interferometer. Checks were performed to assure that no standing wave was present; radiation deflectors destroyed what small standing-wave component existed, so that no change in the Ramsey patterns was observable when changes were made in the phase between the oscillation regions. Figure 8 shows the recorder trace of the observed hyperfine structure. The six Ramsey patterns are shown, although not as clearly as in the case of the interferometer excitation. Peaking of each pattern was possible when observed individually. In Fig. 8, the Ramsey patterns again do not coincide with the intensity maxima but do agree with the frequency measurements obtained in the case of interferometer excitation within the experimental accuracy of the present observations. For the horn-lens excitation, the asymmetry of the patterns resulting from the intensity variation across the pattern limited the frequency measurements to a ± 90-Hz accuracy. Ramsey had indicated that, in the case of short-wavelength traveling waves, frequency shifts cancel for symmetry of the separate field amplitudes about the C-field center, but a shift does occur with asymmetric amplitudes. A severe asymmetry would cause a frequency shift $\delta\nu = 0.027\Delta\nu$ at wavelengths longer than those used here. This corresponds to a frequency shift of 8 Hz in the case of the millimeter observations.

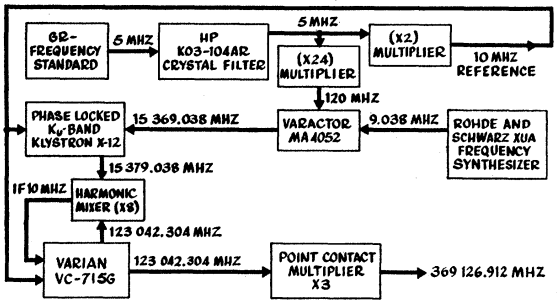

FIG. 9. Multiplying chain for the excitation of the $4_0 \leftrightarrow 4_2$ rotational transition.

Transitions Observed in H_2S

The observation of rotational transitions in hydrogen sulfide was first performed by Burrus and Gordy[11] who measured the two transitions at 168.7 and 216 GHz. During the present investigation, seven H_2S rotational transitions have been observed in millimeter absorption cells. These are listed in Table V. The four transitions, identified by the superscript a, have been observed in the electric-resonance spectrometer. The $2_0 \leftrightarrow 2_2$ transition produced a single line with 290-Hz half-width for the Ramsey pattern. The $3_1 \leftrightarrow 3_3$ transition consists of seven hyperfine components, but sufficient resolution has not as yet been achieved to provide further information on the hyperfine constants. An attempt to observe the $3_{-1} \leftrightarrow 3_1$ transition in the beam apparatus was not successful, presumably owing to an inability to deflect the rotational states sufficiently.

The beam experiments on the $4_0 \leftrightarrow 4_2$ transition at 369 GHz provide electric-resonance observations at the shortest wavelength thus far. The frequency-multiplying chain for these measurements is shown in Fig. 9. The third harmonic of a phase-locked Varian VC-715G klystron at 123 GHz excited the molecular beam. The interferometer constructed for the 168.7-GHz observations was employed for the 369-GHz studies. Low Q and high transmission resulted in a broadened line. Only single-resonator observations were performed. An energy-level diagram of the observed $\Delta m_J = \pm 1$ transitions is shown in Fig. 10. The undisplaced line is observed by Stark modulation at $\nu_0 = 369\,126.912$ MHz and the three Stark components are observed at frequency displacements corresponding to the Stark splittings. Figure 11 shows the zero-field line and the three Stark components. The width of the undisplaced line is approximately 29 kHz; this is a single component with no hyperfine structure. Saturation effects have been checked by detuning the input power but no narrowing of the linewidth has been observed during the tests.

TABLE V. Hydrogen sulfide rotational transitions observed in millimeter-wavelength region.

Transition	Transition frequency (MHz)
$4_0 \leftrightarrow 4_2$[a]	369 126.91±0.1
$2_{-2} \leftrightarrow 2_0$	393 450.40
$3_1 \leftrightarrow 3_3$[a]	300 505.56
$3_{-1} \leftrightarrow 3_1$	369 101.56
$1_{-1} \leftrightarrow 1_1$[a]	168 762.76
$2_0 \leftrightarrow 2_2$[a]	216 710.46
$4_2 \leftrightarrow 4_4$	424 315.47

[a] Observed in electric-resonance spectrometer.

[11] C. A. Burrus and W. Gordy, Phys. Rev. 92, 274 (1953).

TABLE VI. Spin-rotation constants for proton.

Molecule	State	C_H (kHz)	Reference
HDO	2_{20}	−43.47 ±0.11	a
	2_{21}	−43.63 ±0.13	a
HDS	2_{20}	−25.03 ±0.13	a
	2_{21}	−25.45 ±0.13	a
H_2		−113.904±0.030	b
HD		−87.00 ±0.85	c
CH_2O	1_{10}	−0.3	d
	1_{11}	−2.5	d
	2_{11}	+0.65 ±0.50	a
H_2S	1_{10}	−16.239±0.010	This paper
	1_{01}	−15.885±0.010	This paper

[a] P. Thaddeus, L. C. Krisher, and J. H. N. Loubser, J. Chem. Phys. 40, 257 (1964).
[b] N. J. Harrick, R. G. Barnes, P. J. Bray, and N. F. Ramsey, Phys. Rev. 90, 260 (1953).
[c] J. M. B. Kellog, N. F. Ramsey, I. I. Rabi, and J. R. Zacharias, Phys. Rev. 57, 677 (1940).
[d] T. Shiegenari, J. Phys. Soc. Japan 23, 404 (1967).

CONCLUSIONS

The observation of electric resonance in the millimeter-wavelength region has been demonstrated and applied to an asymmetric rotor. The technique provides resolution not previously available for millimeter spectroscopy. The hyperfine constants for the rotational states 1_{10} and 1_{01} of H_2S have been determined, and such a determination should be possible for other polyatomic molecules. Combined with the techniques of beam-maser spectroscopy,[4] the electric-resonance method will permit high-resolution observations on more complicated spectra of molecules.

The techniques which have been described in this paper are applicable to many other molecular transitions occurring in the millimeter-wavelength region. In addition to asymmetric rotors, both symmetric-top mole-

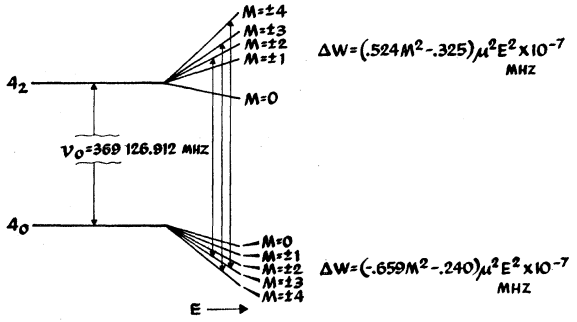

FIG. 10. Energy level configuration: $4_0 \leftrightarrow 4_2$ rotational transition; $\Delta M = \pm 1$ transitions, $\nu_0 = 369\,126.912$ MHz.

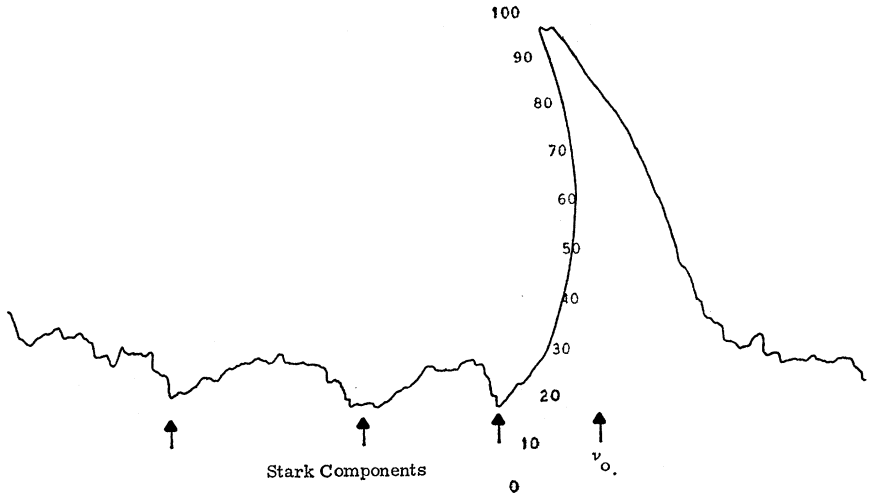

FIG. 11. Recorder trace of the $4_0 \leftrightarrow 4_2$ electric resonance of H_2S at 369 GHz.

cules and diatomic molecules can be investigated. The molecule LiF is being investigated under higher resolution than available in the original millimeter-wave observations.[1] Single interferometer resonances are being observed. The electron bombardment ionizer is replaced by a tungsten hot-wire ionizer in this experiment.

Of particular interest for millimeter molecular-beam investigations are high-temperature and unstable molecules, which are observed with difficulty by conventional millimeter spectroscopy. High-temperature molecular species, such as oxides and hydrides, can be studied by the millimeter molecular-beam methods. The application of the molecular-beam techniques affords several advantages to the millimeter investigations of free radicals. In this apparatus, rotational transitions in metastable electronic states of molecules (e.g., the $^3\pi$ state of CO) can be studied, while symmetric tops with very small dipole moments should provide interesting observations. The molecules CH_3D and CD_3H are examples of the latter case.

The spin-rotation interaction constants $C_{1_{01}}$ and $C_{1_{10}}$ have both been determined to be negative, which is consistent with the results found on several molecules such as H_2, HD, NH_3, HDO, and HDS. For all these molecules, in which the spin-rotation coupling constants are found to be negative, the effect of nuclear frame rotation exceeds that of the electrons. The reasons for this predominance of the nuclear effects are discussed by Shigenari[12] and by White.[13] Recently, the spin-rotation coupling constants $C_{1_{11}}$ for the protons in H_2CO have also been measured to be negative. Only for the state 2_{11} in H_2CO has the constant been measured[4] to be positive. Table VI shows a comparison of the spin-rotation constants for the proton in those molecules for which measurements exist.

The resolution of the $3_1 \leftrightarrow 3_3$ hyperfine structure of H_2S, coupled with the results of Zeeman measurements, would provide further information on the hyperfine structure constants.

The extension of the techniques to shorter submillimeter wavelengths ($\lambda = 812\,\mu$) has been demonstrated. A short-wavelength limit for molecular-beam studies is not evident as long as phase-locked, spectrally pure excitation sources are available. As shorter-wavelength studies are performed, a system of narrow multiple beams will be required for the separated-field method. This is necessary in order to confine the beam to regions of approximately equal amplitude in the two resonators. The effect of a large single beam, as used in the present experiments (0.006 in. wide), at higher frequencies (e.g., $\lambda/2 = 0.010$ in. at 600 GHz) would be to cause molecules to cut regions of different field amplitudes.

ACKNOWLEDGMENTS

This work has been supported by the Solid State and Frequency Control Division, Electronic Components Laboratory, USAECOM, Fort Monmouth, N. J. The authors wish to thank C. Dover, V. E. Derr, and R. Strauch for their assistance and discussions of this problem.

[12] T. Shigenari, J. Phys. Soc. Japan **23**, 404 (1967).
[13] R. L. White, Rev. Mod. Phys. **27**, 276 (1955).